# Optimization of parameter measurement precision with precoupling-assisted weak-value amplification

Manchao Zhang, Jie Zhang ⓘ, Chunwang Wu, Yi Xie ⓘ, Ting Chen ⓘ, Wei Wu, and Pingxing Chen[*]

*Institute for Quantum Science and Technology, College of Science, National University of Defense Technology,*
*Changsha 410073, Hunan, China;*
*Hunan Key Laboratory of Mechanism and Technology of Quantum Information, Changsha 410073, Hunan, China;*
*and Hefei National Laboratory, Hefei 230088, People's Republic of China*

The weak-value amplification is extensively considered in precision metrology in order to achieve a higher sensitivity. Despite the practical benefits in amplifying small physical quantities, its metrological advantage still arouses a broad debate due to the low postselection probability of success. In this paper, by employing the quantum Fisher information metric, we show that the precision of estimating an unknown parameter can be improved by introducing a precoupling process with properly chosen interaction operators. We point out this result is credible for both real and imaginary weak values. By tracking the meter wave functions, we find this enhancement of estimation precision comes from a precoupling induced modulation of the meter wave function, thus the most sensitive regime with respect to the parameter is reached. In addition, the estimation error is investigated by considering the difference between the theoretical and estimated value. The analysis suggests that this kind of error can be effectively suppressed by averaging the estimations resulted from different initial meter states. These results are finally illustrated by an exact numerical simulation where the advantages of our proposal are displayed by the comparison to the standard weak-value amplification scheme.

## I. INTRODUCTION

The precision measurement of weak physical quantities, such as the strength of the magnetic field, is essential for exploring physical effects [1,2]. Following a general scheme, the quantity can be mapped to the change of system quantum states and then extracted by a designed state detection and postprocessing. Through this procedure, one usually expects to estimate the quantity with smallest possible uncertainty by utilizing limited quantum resources, to be more specific, to achieve higher signal-to-noise ratio (SNR) [3–5] or Fisher information (FI) [6–8].

The concept of weak-value amplification (WVA) [9,10] proposed by Aharonov, Albert, and Vaidman (AAV) has attracted broad attention due to its practical potential in detecting tiny effects [11–13]. The WVA scheme involves a weak coupling between the target system and a meter. Because of the postselection operation, the average shift rate of the meter wave packet can go far beyond the maximum eigenvalue of the observable [14,15]. Therefore, when compared to the conventional measurement (CM), one would say that the WVA scheme provides an enhanced sensitivity of estimating ultrasmall parameters. However, this statement has sparked widespread controversy in some articles [16,17] for the reason that the WVA with higher FI inevitably comes with a reduced postselection probability of success. This indicates a large portion of the output data is discarded, which in turn cancels

the benefits of the amplification effect. And it is shown that the failed postselection events also possess a small portion of FI, which will generally lead to a loss of estimation precision. But surprisingly, some studies suggest that the WVA technique may outperform the CM as well if systematic imperfection exists [18,19]. For example, when the WVA is employed against the detector saturation, one can achieve a precision six times higher than that of CM [19]. Also, it has been pointed out that the technical noise can be suppressed by the WVA technique in some circumstances [20–25], and even the SNR may be increased by several orders of magnitude via imaginary weak-value measurements [23,24]. As an example, in Ref. [25], the authors suggest that with WVA, the systematic error induced by the decoherence on the meter can be reduced because the interaction parameter is amplified while the noise is not.

Although the metrological power of WVA is debated, considering the amplifying effect in detecting tiny physical quantities, the attempts aiming to improve its performance are still significant. For instance, to address the problem of low postselection probability [26], Pang and Brun [27] pointed out that by optimizing the initial and postselected states to maximize either postselection probability or weak value, the loss of FI can be negligible. And Dressel *et al.* [28] and Krafczyk *et al.* [29] have suggested to recycle the postselection rejected events to avoid information loss. Whereafter, Strübi and Bruder [30], Martínez-Rincón *et al.* [31], Qin and Li [32], and Huang *et al.* [33] adopted this idea and then developed the joint weak-value amplification and dual weak-value amplification techniques, respectively. Additionally, it is found that by adding quantum resources one can

*pxchen@nudt.edu.cn

also improve the estimation precision [4,5,34,35]. On the one hand, the nonclassical quantum states of meters such as squeezed states are proven to be more powerful in the WVA-based metrology than classical states [4,5], which is consistent with the expectation of quantum resource theory [36]. Meanwhile, from the aspect of the system, studies indicate that using a $N$-partite entangled system also provides such a precision improvement, and has the capacity to achieve the Heisenberg-limited precision scaling [34,35]. It should be mentioned that this improvement is in fact resulted from the $N$-fold postselection probability increase while the amplification factor is preserved. For the above proposals, however, Kim *et al.* [37] pointed out the possible challenges in preparing the nonclassical meter states or macroscopic entangled quantum states. Then they proposed and demonstrated a novel WVA scheme based on iterative interactions, by which they also achieved the Heisenberg-limited precision scaling but no entanglement state was used.

Recently, Zhang *et al.* [38] proposed a biased weak-value amplification (BWVA) technique for measuring small longitudinal phase change by introducing an extra bias phase. Because the extra phase initializes the joint system into an optimal work regime, they concluded that the BWVA can result in sensitivity outperforming the standard WVA by two orders of magnitude at the expense of lower signal density. This scheme is then employed by Yin *et al.* [39] to achieve precision improvement of optical metrology in the presence of saturation effect. Note that the BWVA is actually equivalent to the WVA scheme working beyond the AAV limit [24], which leads to limited applications.

In this paper, we propose a general precoupling-assisted weak-value amplification (PWVA) technique. To make the model universally valid for various practical circumstances, we make no assumption about the form of precoupling and weak-interaction operations. During the formula derivation process, the linear approximation with respect to the coupling strength is adopted in order to simplify the results, as most papers do. We find that due to the extra precoupling which causes entanglement between system and meter, the state-dependent wave functions of the meter are modulated, thus the most sensitive regime with respect to $g$ is reached. After the wave-packet interference, the postselection probability and changing rate of the meter wave packet are optimized. And as a result, an improved estimate precision is achieved if the precoupling process is properly designed. Additionally, according to the comparison of estimation error between PWVA and WVA, an optimized method based on averaging the estimation results derived from different initial states or weak values is also provided. We note that compared to WVA, PWVA does not need extra quantum resources such as squeezing or entanglement with other systems. This actually indicates wider application in high-resolution experiments. The remainder of this paper is organized as follows. In Sec. II we briefly review the WVA-based metrology and show its estimation precision with the metric of FI. In Sec. III, a general PWVA theoretical model is derived. By the FI calculation, the higher metrological power of PWVA than WVA is shown. Then a numerical example comparing the PWVA and WVA is given in Sec. IV. Finally, we conclude in Sec. V.
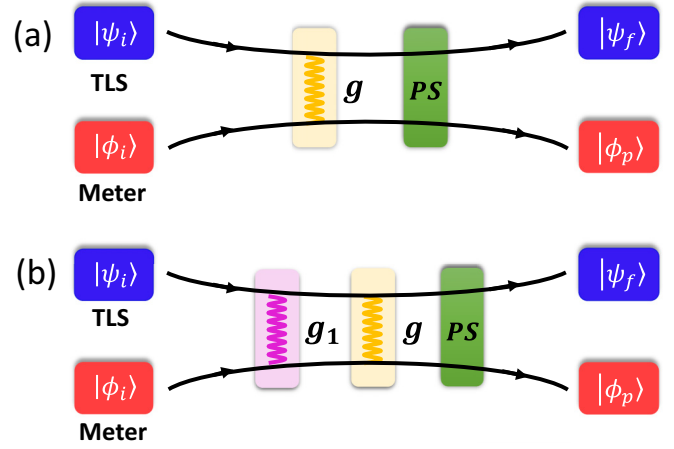


FIG. 1. Two WVA schemes aiming to estimate a parameter $g$ by the interaction between a TLS and meter. (a) The standard WVA. The meter is detected after interacting with a TLS with strength $g$ and experiencing a postselection procession (PS). (b) The precoupling-assisted WVA. Compared to the standard WVA scheme, an additional precoupling operation is applied after the state initialization.

## II. REVIEW OF THE WVA THEORY

The principle of the standard WVA scheme is depicted in Fig. 1(a) where the two-level system (TLS) and measuring device (meter) are initially prepared in states $|\psi_i\rangle$ and $|\phi_i\rangle$, respectively. Then they are coupled by an interaction Hamiltonian modeled by ($\hbar = 1$ throughout the paper)

$$H = gA \otimes \Omega\delta(t - t_0), \tag{1}$$

where $A$ and $\Omega$ are observables of the TLS and meter, and $g$ characterizes the coupling strength. The $\delta$ function indicates that the interaction is instantaneous at time $t_0$. After this interaction, if the TLS is postselected to state $|\psi_f\rangle$, the meter collapses to (un-normalized)

$$|\phi\rangle = \langle\psi_f|\exp(-igA \otimes \Omega)|\psi_i\rangle|\phi_i\rangle.$$

It can be simplified when $g \ll 1$:

$$
\begin{aligned}
|\phi\rangle &\approx \langle\psi_f|(I - igA \otimes \Omega)|\psi_i\rangle|\phi_i\rangle \\
&= \langle\psi_f|\psi_i\rangle(I - igA_w\Omega)|\phi_i\rangle, \tag{2}
\end{aligned}
$$

where $A_w$ is the weak value, defined as

$$A_w = \frac{\langle\psi_f|A|\psi_i\rangle}{\langle\psi_f|\psi_i\rangle}. \tag{3}$$

When $\langle\psi_f|\psi_i\rangle \to 0$, $A_w$ can be very large (strongly violating the bounds of the eigenvalues of $A$), leading to an amplifying effect. But this requires a very small overlap between the states $|\psi_i\rangle$ and $|\psi_f\rangle$. When $g$ is very small so that $gA_w \ll 1$ holds, the success probability of postselection is approximately

$$P^S \approx |\langle\psi_f|\psi_i\rangle|^2. \tag{4}$$

Then the normalized meter state after postselection can be written as

$$|\phi_p\rangle = |\phi\rangle/\sqrt{P^S} \approx \exp(-igA_w\Omega)|\phi_i\rangle, \quad (5)$$

a $g$-dependent pure state.

When repeating $N$ independent WVA operations, the minimum achievable variance of the estimator $g$ based on analyzing state $|\phi_p\rangle$ is given by the Cramér-Rao bound [6]: $\langle(\delta g)^2\rangle \geqslant \frac{1}{NF_I} + \langle\delta g\rangle^2$. The first term on the right side is the inverse of classical Fisher information (CFI) and scales as $N^{-1}$. The second term $\langle\delta g\rangle^2$, representing the systematic error, is independent of $N$, which implies this term cannot be suppressed by increasing the repeating number $N$. Typically, the CFI is a powerful tool for the parameter estimation about a parameter $g$. It is a function of the conditional probability distribution $f(z|g)$ obtained by measuring the quantum state, and is defined as $F_I[f(z|g)] = P^S \int dz \frac{1}{f(z|g)}[\partial_g f(z|g)]^2$ with $P^S$ the postselection probability. It should be mentioned that the CFI is always positive and is upper bounded by the quantum Fisher information (QFI). The latter can be attained by optimizing the measurement scheme. In quantum metrology, the QFI determines the precision limit about the parameter estimation:

$$\langle(\delta g)^2\rangle \geqslant \frac{1}{NQ_I} + \langle\delta g\rangle^2. \quad (6)$$

For a pure state, QFI can be expressed as $4P^S(\langle\partial_g\phi_p|\partial_g\phi_p\rangle - |\langle\phi_p|\partial_g\phi_p\rangle|^2)$ [6,7]. Therefore, combined with Eqs. (4) and (5), it is clear that the QFI depends on states $|\psi_i\rangle$ as well as $|\psi_f\rangle$. And its achievable maximum reads $Q_I^S = 4\text{Var}(\Omega)$ with $\text{Var}(\Omega)$ the variance of $\Omega$ in the state $|\phi_i\rangle$, equaling to the optimized QFI of the CM scheme. This result confirms that although the postselected events possess remarkable sensitivity, WVA offers no metrological advantages over CM due to the necessarily reduced postselection probability of success.

### III. PRECOUPLING WVA THEORY

In this section, a general theoretical model of the PWVA scheme is introduced. PWVA is a parameter metrology developed from the WVA method. Their difference lies on the precoupling operation after the state initialization stage of both TLS and meter [Fig. 1(b)]. The precoupling process is realized by an interaction Hamiltonian:

$$H_1 = g_1 A \otimes \Omega_1 \delta(t - t_1). \quad (7)$$

Similar to $H$, $g_1$ represents the coupling strength. $A$ and $\Omega_1$ are operators acting on the TLS and meter, respectively. To simplify the model, we assume the operator $A$ in $H$ and $H_1$ remains the same, while $\Omega_1$ usually differs from $\Omega$ to ensure the flexibility in designing an experimental scheme. As a result of the precoupling described by a unitary operator $U_1 = \exp(-ig_1 A\Omega_1)$, the TLS and meter are entangled. It is equivalent to updating the initial state of WVA. Therefore, the quantum state of the combined system before postselection can be written as

$$|\Psi\rangle = \exp\{-igA \otimes \Omega\}\exp\{-ig_1 A \otimes \Omega_1\}|\psi_i\rangle|\phi_i\rangle. \quad (8)$$

Supposing $g, g_1 \ll 1$ and $g_1 \geqslant g$, expand the equation and ignore the nonlinear terms of $g$, then we have

$$|\Psi\rangle \approx (I - igA \otimes \Omega)\left(\sum_{k=0}^{\infty} \frac{1}{k!}(-ig_1)^k A^k \otimes \Omega_1^k\right)|\psi_i\rangle|\phi_i\rangle$$

$$= \left[\sum_{k=0}^{\infty} \frac{1}{k!}(-ig_1)^k A^k \otimes \Omega_1^k \right.$$

$$\left. - g\sum_{k=0}^{\infty} \frac{1}{k!}(-i)^{k-1}g_1^k A^{k+1} \otimes \Omega\Omega_1^k\right]|\psi_i\rangle|\phi_i\rangle. \quad (9)$$

After this interaction, if the TLS is postselected to state $|\psi_f\rangle$, the meter will collapse to a normalized pure state:

$$|\phi_p^{(v)}\rangle \approx \frac{1}{\sqrt{r_P^{(v)}}}|\phi^{(v)}\rangle$$

$$= \frac{1}{\sqrt{r_P^{(v)}}}\left[\sum_{k=0}^{v} \frac{1}{k!}(-ig_1)^k(A^k)_w\Omega_1^k \right.$$

$$\left. - g\sum_{k=0}^{v} \frac{1}{k!}(-i)^{k-1}g_1^k(A^{k+1})_w\Omega\Omega_1^k\right]|\phi_i\rangle. \quad (10)$$

Here, $v$ represents the truncation index of $k$. $(A^k)_w = \langle\psi_f|A^k|\psi_i\rangle/\langle\psi_f|\psi_i\rangle$ is defined as the generalized weak value and Eq. (3) shows a special example when $k = 1$. $r_P^{(v)} = P^{(v)}/|\langle\psi_f|\psi_i\rangle|^2 = \langle\phi^{(v)}|\phi^{(v)}\rangle$ indicates the relative postselection probability between PWVA and WVA [Eq. (4)]:

$$r_P^{(v)} = c_0^{(v)} + c_1^{(v)}g + o(g^2), \quad (11)$$

where the coefficients read

$$c_0^{(v)} = 1 + \sum_{k,l=0,k+l>0}^{k+l\leqslant v} \frac{1}{k!l!}g_1^{k+l}(A^k)_w^*(A^l)_w\langle\Omega_1^{k+l}\rangle,$$

$$c_1^{(v)} = 2\sum_{k,l=0,k+l\geqslant0}^{k+l\leqslant v} \frac{1}{k!l!}g_1^{k+l}\text{Re}\big[i^{k-l-1}(A^k)_w^*(A^{l+1})_w$$

$$\times \langle\Omega_1^k\Omega\Omega_1^l\rangle\big].$$

For simplicity, we denote $\langle\phi_i|O|\phi_i\rangle$ as $\langle O\rangle$ for short throughout the paper where O represents an arbitrary operator in meter system. Because the QFI of state $|\phi^{(v)}\rangle/\sqrt{r_P^{(v)}}$ can be written as

$$Q_I^{(v)} = 4P^{(v)}\big[\langle\partial_g\phi^{(v)}|\partial_g\phi^{(v)}\rangle/r_P^{(v)} - |\langle\phi|\partial_g\phi\rangle|^2/(r_P^{(v)})^2\big].$$

We finally obtain

$$Q_I^{(v)} = \frac{4|\langle\psi_f|A|\psi_i\rangle|^2}{r_P^{(v)}}\left\{\text{Var}(\Omega) + \sum_{k,l=0,k+l>0}^{k+l\leqslant v} \frac{1}{k!l!}i^{k-l}g_1^{k+l}\right.$$

$$\left. \times (A^k)_w^*(A^l)_w\big[\langle\Omega^2\rangle\langle\Omega_1^{k+l}\rangle - \langle\Omega_1^k\Omega\rangle\langle\Omega\Omega_1^l\rangle\big]\right\}. \quad (12)$$

This expression shows the main result of this paper. One of its simplified forms can be obtained by setting $g_1 \approx g$ (linear

region) so that $v = 1$ can provide a very good approximation of Eq. (12).

(i) If $A_w \in \mathbb{R}$, then $r_P^{(1)} \approx 1$, and

$$Q_I^{(1)} \approx Q_I^S + 4|\langle\psi_f|A|\psi_i\rangle|^2(-ig_1 A_w \langle\Omega\rangle\langle[\Omega_1, \Omega]\rangle), \quad (13)$$

where $[\Omega_1, \Omega]$ represents the commutation relation between operators $\Omega_1$ and $\Omega$. The first term $Q_I^S = 4|\langle\psi_f|A|\psi_i\rangle|^2\text{Var}(\Omega)$ provides the QFI of WVA. In this case, we see that the QFI can be increased only when the requirement $[\Omega_1, \Omega] \neq 0$ is met. This provides us with criteria to select suitable operators for experimental design. For example, when $\Omega = p$, the momentum operator, it is positive to select the position operator $x$ or number operator $n$ as $\Omega_1$. The choice $\Omega_1 = \Omega = p$, i.e., applying WVA technique beyond the AAV limit, however, would be unavailing, so it should be avoided in practice.

(ii) If $A_w/i \in \mathbb{R}$, $r_P^{(1)} = 1 + 2\text{Im}(A_w)(g\langle\Omega\rangle + g_1\langle\Omega_1\rangle)$, then $r_P^{(1)} \approx 1 - 2\text{Im}(A_w)(g\langle\Omega\rangle + g_1\langle\Omega_1\rangle)$, we obtain

$$Q_I^{(1)} \approx Q_I^S + 4|\langle\psi_f|A|\psi_i\rangle|^2[g_1\text{Im}(A_w)\langle\Omega\rangle(2\langle\Omega\rangle\langle\Omega_1\rangle \\ - \langle\{\Omega_1, \Omega\}\rangle)], \quad (14)$$

where $\{\Omega_1, \Omega\}$ is the anticommutation relation of $\Omega_1$ and $\Omega$. And the WVA's QFI reads $Q_I^S = 4|\langle\psi_f|A|\psi_i\rangle|^2\{\text{Var}(\Omega)[1 - 2g\text{Im}(A_w)\langle\Omega\rangle]\}$. Differing from case (i), this scenario possesses more freedom in QFI optimization. For example, supposing that $\Omega = \Omega_1 = p$, then $Q_I^{(1)} = Q_I^S - 4|\langle\psi_f|A|\psi_i\rangle|^2 2g_1\text{Im}(A_w)\text{Var}(p)$. Therefore the condition $\text{Im}(A_w) < 0$ will lead to an improvement of QFI, which is incompatible with the result obtained in (i). This different performance of QFI suggests that the parameter setting plays a crucial role in the PWVA-based metrology. It is worth noting that the condition $\Omega = \Omega_1$ in PWVA is actually equivalent to the increase of interaction strength $g$ to $g + g_1$ in WVA, a special scenario corresponding to the BWVA scheme studied in Refs. [38,39].

The discussion above shows an impressive metrological performance of PWVA over WVA. Note that despite the assumption $g_1 \approx g$, this conclusion is still credible when we extend the precoupling strength $g_1$ to a more general range $g_1 \geqslant g$. The only expense we have to pay is the increased complexity for the QFI derivation with a higher $v$. But why is precoupling more beneficial to improve the QFI? In the following, we will explore this by a further consideration on the definition of CFI. Beginning from the initial state $|\phi_i\rangle$ with probability distribution $f(z)$, after the interaction and postselection, the shape of the wave packet is largely distorted, and as a result, its central location is shifted by $\Delta(g)$. Suppose a general probability distribution $h(z) = f[z - \Delta(g)] + \widetilde{f}[z|\Delta(g)]$ of $|\phi_p\rangle$, where $f[z - \Delta(g)]$ illustrates the part shifted from the initial state $f(z)$, meaning that the shape of the meter is not changed. The second term $\widetilde{f}[z|\Delta(g)]$ shows the deformation degree and satisfies $\int dz \widetilde{f}[z|\Delta(g)] = 0$. In general, this term appears if the precoupling strength is large enough or when the WVA technique works beyond the AAV limit. Then the CFI transforms to

$$F_I[h(z)] = P \int dz \frac{\{\partial_g f[z - \Delta(g)] + \partial_g \widetilde{f}[z|\Delta(g)]\}^2}{f[z - \Delta(g)] + \widetilde{f}[z|\Delta(g)]}. \quad (15)$$

Here, we cannot proceed any further derivation without a definite expression of $h(z)$. But Eq. (15) still reveals three possible factors that may contribute to the enhancement of Fisher information. One is the postselection probability $P$. In precision metrology, the information gained about $g$ is proportional to the number of successful events. For a certain $N$, it will be helpful if $P$ is optimized. The other refers to the shift $\Delta(g)$ or its differential defined as $R_S = |\partial_g \Delta(g)|$. $R_S$ acts as the shift rate at which the central location of $h(z)$ changes as $g$, and a larger $R_S$ usually means a higher sensitivity of a single postselected trial when measuring $g$. Taking $\Omega = p$ for example, when the deformation effect $\widetilde{f}[z|\Delta(g)](z = x$ or $p)$ of the wave packet is negligible compared to $R_S$, the wave packet only experiences a shift from the initial location. Define $z' = z - \Delta(g)$, then the derivative with respect to $g$ can be modified by the chain rule $\partial_g f[z - \Delta(g)] = -\partial_g \Delta(g)\partial_{z'} f(z')$. As $dz' = dz$ with the same integral interval under the change of integration variable, then Eq. (15) reduces to

$$F_I[h(z)] = PR_S^2 \int dz' \frac{[\partial_{z'} f(z')]^2}{f(z')}, \quad (16)$$

where $\int dz' [\partial_{z'} f(z')]^2/f(z')$ implies the metrological power of initial state $|\phi_i\rangle$. And most importantly, the CFI is proportional to the square of $R_S$. Note that Eq. (16) actually corresponds to the FI of WVA where no deformation effect occurs. By optimizing $P$ and measurement basis, we will find the QFI is upper bounded by $Q_I^S = 4\text{Var}(\Omega)$, a quantity determined by the characteristics of the initial state. For the PWVA scheme, however, a much larger $R_S$ or $P$ can be achieved, which finally yields a QFI beyond $Q_I^S$. One example illustrating this can be found in Fig. 2, the numerical results for the case $A_w = -20i$. In addition, the QFI increase may be also rooted in the deformation term $\widetilde{f}[z|\Delta(g)]$. On the one hand, $\widetilde{f}[z|\Delta(g)]$ is associated with $\Delta(g)$. The properties of $\Delta(g)$ are partially characterized by the behavior of $\widetilde{f}[z|\Delta(g)]$. On the other hand, although $R_S$ may approach zero under particular parameter settings, the sensitive response of $\widetilde{f}[z|\Delta(g)]$ to $g$ still ensures the QFI enhancement. This can be shown by assuming $R_S = 0$, then

$$F_I[h(z)] = P \int dz \frac{[\partial_g \widetilde{f}(z|g)]^2}{f(z) + \widetilde{f}(z|g)}. \quad (17)$$

This means that a higher deformation rate can lead to a higher FI. One example illustrating this will be shown in Fig. 2 too, i.e., the regime enclosed by green dashed rectangles. Finally, we emphasize that all three indices listed above are somewhat dependent on each other. One needs to make a compromise among them for realizing an optimal performance of PWVA.

We next provide a detailed analysis of $R_S$ to show its contribution to QFI. In the PWVA-based metrology, it is clear that after postselection the average location of the meter wave packet with respect to an observable $M$ is given by $\langle\phi^{(v)}|M|\phi^{(v)}\rangle/r_P^{(v)}$, which yields

$$\langle M \rangle_p^{(v)} = \frac{d_0^{(v)} + d_1^{(v)}g}{c_0^{(v)} + c_1^{(v)}g} + o(g^2) \quad (18)$$
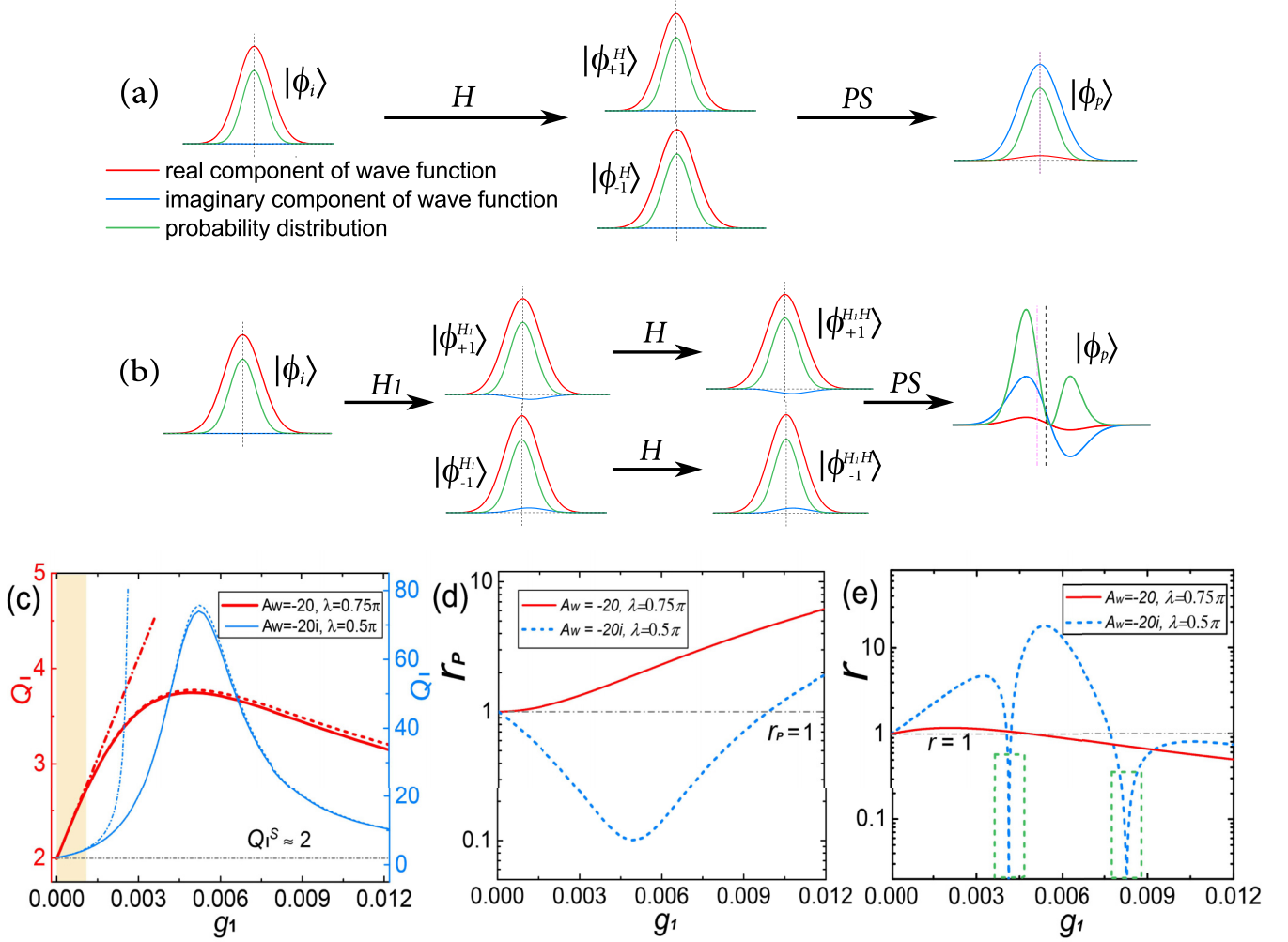
FIG. 2. The metrological advantages of PWVA over WVA. (a), (b) The tracking of the meter wave functions of both WVA and PWVA schemes. The black and purple dashed vertical lines represent the average location of states before and after postselection operation, respectively. (c) The QFI as a function of $g_1$ ($g = 10^{-4}$). This figure is plotted with two independent $y$ axes. The one in red (thick curves) shows the QFI behavior with the initial state $s = 3$, $\lambda = 0.75\pi$ and the weak value $A_w = -20$. The blue one (thin curves) corresponds to the parameters setting $s = 3$, $\lambda = 0.5\pi$, $A_w = -20i$. Their results are marked in three types of curves: the exact numerical solutions with solid curves, $v = 1$ with the dot-dashed curves, and $v = 2$ with the dashed curves. The region marked in light orange shows the linear response of QFI to $g_1$, corresponding to the approximate solutions Eqs. (13) and (14). (d) The relative postselection probability $r_P$ of success. (e) The performance of the relative wave-packet shift rate $r$ as $g_1$ changes. The green dashed boxes identify the regime that should be avoided in PWVA technique. It should be pointed out that, for comparison, the QFI, $r_p$, and $r$ of the WVA scheme are shown by the gray dot-dashed lines in (c), (d), and (e), respectively. In figures (d) and (e), the red solid curves and blue dashed curves are resulted from the same parameters as in (c).

with the definitions

$$d_0^{(v)} = \langle M \rangle + \sum_{\substack{k,l=0,k+l>0}}^{k+l \leqslant v} \frac{1}{k!l!} g_1^{k+1} (A^k)_w^* (A^l)_w \langle \Omega_1^k M \Omega_1^l \rangle,$$

$$d_1^{(v)} = 2 \sum_{\substack{k,l=0 \\ k+l \geqslant 0}}^{k+l \leqslant v} \frac{1}{k!l!} g_1^{k+l} \mathrm{Re}\big[ i^{k-l-1} (A^k)_w^* (A^{l+1})_w \langle \Omega_1^k M \Omega \Omega_1^l \rangle \big].$$

Then the meter shift can be obtained by the calculation $\Delta(g) = \langle M \rangle_p^{(v)} - \langle M \rangle$ and the shift rate $R_S$ is also available.

Let us consider the weak precoupling condition $g_1 \approx g$, where the spread of the meter wave function is almost unchanged and the Hamiltonians $H$ and $H_1$ only result in a shift of the wave packet in the phase space. The direction of this

shift mainly depends on the operators $\Omega$ and $\Omega_1$ and also the weak value $A_w$. In the first-order approximation with respect to $g$ and $g_1$, the relative postselection probability is given by $r_P^{(1)} = c_0^{(1)} + c_1^{(1)} g \approx 2 - c_0^{(1)} - c_1^{(1)} g$. Then the shift rate $R_S^{(1)}$ is approximately

$$R_S^{(1)} \approx \big| 2d_1^{(1)} - c_0^{(1)} d_1^{(1)} - c_1^{(1)} d_0^{(1)} \big|. \tag{19}$$

Taking $A_w \in \mathbb{R}$ for example, then Eq. (19) can be simplified to

$$R_S^{(1)} \approx \big| - i A_w \langle [M, \Omega] \rangle + g_1 A_w^2 (2\mathrm{Re}[\langle \Omega_1 M \Omega \rangle] - \langle M \rangle \langle \{\Omega_1, \Omega\} \rangle) \big|. \tag{20}$$

To make a comparison, we introduce $R_S^S = \big| - i A_w \langle [M, \Omega] \rangle \big|$ as the shift rate of WVA. If $M = x$, $\Omega = p$, $\Omega_1 = x$,

and $A_w > 0$, then we have $R_S^S = A_w$, while $R_S^{(1)} = A_w + 2g_1 A_w^2 \text{Re}[\langle x^2 p \rangle - \langle x \rangle \langle xp \rangle]$. When the initial state $|\phi_i\rangle$ meets the condition $\langle p \rangle > 0$, a desired result occurs that $R_S^{(1)} > R_S^S$, which implies a higher QFI over WVA and is consistent with the previous discussion in case (i).

A notable point here is that as $g_1$ grows, Eq. (19) is no longer accurate. The nonlinear terms of $g_1$ start to play a significant role in the PWVA technique. This expects us to carefully choose a higher but not too large truncation index $v$ for the reason that a larger $v$ usually acts as a double-edged sword. That is, the increase of $v$ may effectively enhance the measurement precision of $g$, but meanwhile, it will bring more complicated calculation. In addition, despite the well-performed shift rate $R_S$, a larger $g_1$ may lead to deformation of the wave packet or reduction of the postselection probability as well. One needs to take all the factors into consideration when analyzing the reasons why PWVA may outperform the standard WVA with respect to a metrological purpose.

## IV. NUMERICAL EXAMPLE

To illustrate the results derived in Sec. III, we use a numerical computation to show the effect of precoupling in the PWVA metrology. Without loss of generality, we assume $\Omega \neq \Omega_1$, and the Hamiltonians are $H = g\sigma_z \otimes p\delta(t - t_0)$ and $H_1 = g_1\sigma_z \otimes n\delta(t - t_1)$, where $\sigma_z$ represents an atomic Pauli operator expressed as $\sigma_z = |\uparrow\rangle\langle\uparrow| - |\downarrow\rangle\langle\downarrow|$. $n = a^\dagger a$ is the number operator with $a^\dagger$ ($a$) the creation (annihilation) operator. Here, we introduce the quadratures $X_\mu = i(e^{-i\mu}a^\dagger - e^{i\mu}a)/\sqrt{2}$ with $\mu \in [0, 2\pi)$ to give the definition of momentum and position operators: $p = X_0 = i(a^\dagger - a)/\sqrt{2}$ and $x = X_{\pi/2} = (a^\dagger + a)/\sqrt{2}$. As one can easily check, the commutation relation $[x, p] = i$ still holds.

Considering the purpose of the WVA-based precision metrology, we usually desire $|A_w|$ to be much larger than the maximum eigenvalue of $A$. In this case, the largest postselection probability of success for a given weak value $A_w$ was shown to be $\approx \text{Var}(A)_{|\psi_i\rangle}/|A_w|^2$ [27], where $\text{Var}(A)_{|\psi_i\rangle}$ is the variance of operator $A$ in the initial state $|\psi_i\rangle$ of the TLS. Therefore, in order to reach the optimal QFI, we assume that the TLS is initially prepared in a superposition state $|\psi_i\rangle = (|\uparrow\rangle + |\downarrow\rangle)/\sqrt{2}$. And the postselection state is set to be a generalized state characterized by $|\psi_f\rangle = \cos(\frac{\theta}{2})|\uparrow\rangle + \exp(i\varphi)\sin(\frac{\theta}{2})|\downarrow\rangle$, with the Bloch-vector polar angles $\theta \in [0, \pi]$ and $\varphi \in [0, 2\pi)$. Depending on $|\psi_i\rangle$ and $|\psi_f\rangle$, the weak value reads as $A_w = [1 - \tan(\theta)e^{-i\varphi}]/[1 + \tan(\theta)e^{-i\varphi}]$.

Suppose the initial state of the meter is $|\phi_i\rangle = |\alpha\rangle$, a coherent state with $\alpha = se^{i\lambda} \in \mathbb{C}$. By utilizing the properties $\exp(-img_1 n)|\alpha\rangle = |\alpha_m\rangle = |\alpha e^{-img_1}\rangle$ and $\exp(-igX_0) = D(g/\sqrt{2})$, where $D(\alpha) = \exp(\alpha a^\dagger - \alpha^* a)$ is a displacement operator, the entanglement state of the combined system after precoupling can be expressed as

$$|\Psi_1\rangle = \frac{1}{\sqrt{2}}[|e\rangle|\phi_{+1}^{H_1}\rangle + |g\rangle|\phi_{-1}^{H_1}\rangle]$$

$$= \frac{1}{\sqrt{2}}[|e\rangle|\alpha e^{-ig_1}\rangle + |g\rangle|\alpha e^{ig_1}\rangle]. \quad (21)$$

Due to the interaction $H$, $|\Psi_1\rangle$ evolves to

$$|\Psi\rangle = \frac{1}{\sqrt{2}}[|e\rangle|\phi_{+1}^{H_1 H}\rangle + |g\rangle|\phi_{-1}^{H_1 H}\rangle],$$

where $|\phi_m^{H_1 H}\rangle = \exp[-i\frac{gs}{\sqrt{2}}\sin(g_1 - m\lambda)]|\frac{mg}{\sqrt{2}} + \alpha_m\rangle$ with $m = \pm 1$. Then the meter's un-normalized state after postselection can be written as

$$|\phi\rangle = \frac{1}{\sqrt{2}}\left[\cos\left(\frac{\theta}{2}\right)|\phi_{+1}^{H_1 H}\rangle + e^{-i\phi}\sin\left(\frac{\theta}{2}\right)|\phi_{-1}^{H_1 H}\rangle\right]. \quad (22)$$

Equation (22) indicates that after the postselection, the meter state is a superposition of $|\phi_{+1}^{H_1 H}\rangle$ and $|\phi_{-1}^{H_1 H}\rangle$ with the postselection probability of success $P = \langle\phi|\phi\rangle$.

In Fig. 2(c), we display a numerical result concerning the dependence of QFI on the precoupling strength $g_1$. To verify the conclusion predicted by the approximate solutions, i.e., Eqs. (13) and (14), we employ an initial meter state cooperated with a real or pure imaginary weak value to calculate the QFI. As expected, in the light orange marked area, the QFI is proportional to $g_1$ (dot-dashed curves, $v = 1$), which is consistent with the predicted linear response. But as $g_1$ grows, the model tends to be nonlinear, and $Q_I^{(1)}$ starts to diverge from the exact numerical results (solid curves). Instead, the $Q_I^{(2)}$ (dashed curves) varies approximately parabolically with $g_1$, leading to a smaller difference. This improvement is associated with the correction by the second-order terms of $g_1$ in $Q_I^{(2)}$. And it is clear that the numerical calculation will be more accurate when the higher-order terms are included. We emphasize that except for the results above, the most remarkable feature in Fig. 2(c) is the greatly increased QFI of PWVA compared to $Q_I^S \approx 2$, the maximum achievable QFI of WVA. This enables us to realize a more efficient precision metrology by using PWVA, which of course depends heavily on a proper setting of parameters such as $|\phi_i\rangle$, $g_1$, and $A_w$.

Next, the relative postselection probability $r_p$ and relative wave-packet shift rate $r = R_S/|A_w|$ are investigated in Figs. 2(d) and 2(e), respectively. We conclude that under different parameter settings, the contributions from $r_P$ or $r$ to the QFI increase may be significantly different. For example, by selecting a pure imaginary $A_w$ and observable $M = p$, a lower postselection probability is produced, while the wave-packet shift becomes much more sensitive to the measured parameter $g$ (blue dashed curves). This means the remarkable QFI here mainly comes from $r$. In contrast, there also exist some cases where the QFI mainly benefits from the increased postselection probability, such as the scenario $A_w \in \mathbb{R}$ illustrated by the red curves. Note that in the interval of $g_1$ enclosed by the green dashed boxes in Fig. 2(e), $r$ is smaller than 1 and even approaches zero, implying a smaller shift rate than WVA. Combined with Figs. 2(c) and 2(d), we conclude that the metrology advantage of PWVA in this region is mainly rooted in the deformation effect. Therefore, if one aims to estimate $g$ based on the central location of $|\phi_p\rangle$, when considering the limited resolution of the detector, we suggest that $g_1$ should be chosen outside this area and following the criteria: $r \geqslant 1$. As for $Q_I$, of course, the higher the better.

Here, we provide a physical interpretation of the QFI enhancement shown in Figs. 2(c)–2(e) by tracking the meter wave functions. In the WVA scheme [see Fig. 2(a)], because
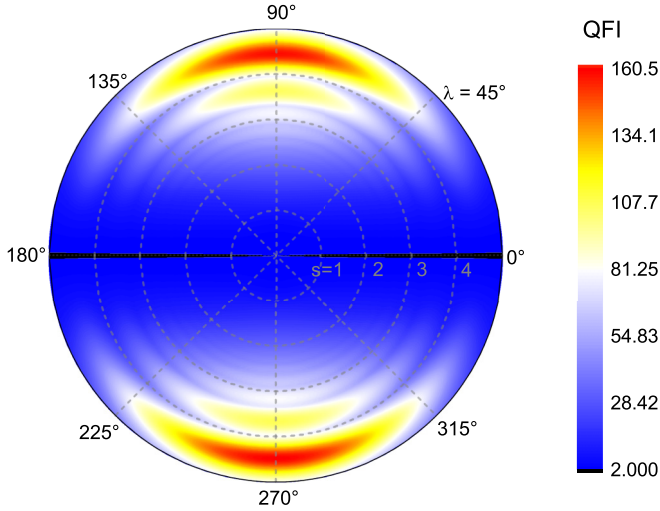
FIG. 3. The contours of optimized QFI obtained by scanning $A_w$ for the initial coherent states $|se^{i\lambda}\rangle$ with $s \in [0, 5]$ and $\lambda \in [0, 2\pi)$. In the small black region along the horizontal axis with $\lambda = 0$ and $\pi$, we obtain $Q_I < 2$. This indicates that the PWVA possesses no metrological advantages over WVA when the operator $\Omega = p$. Other parameters used in the calculation are $g = 10^{-4}$ and $g_1 = 0.005$.

the interaction $H$ is weak, the state-dependent wave functions $|\phi_{+1}^H\rangle$ and $|\phi_{-1}^H\rangle$ only slightly differ from the initial state $|\phi_i\rangle$. As a result, except for a small shift, the probability distribution of the final state $|\phi_p\rangle$ is almost unchanged, which results in limited estimation precision. For our PWVA scheme [see Fig. 2(b)], however, due to the precoupling operation, $|\phi_{+1}^{H_1}\rangle$ and $|\phi_{-1}^{H_1}\rangle$ are modulated. They are largely deformed from the initial state $|\phi_i\rangle$ and the difference between their imaginary components becomes quite evident. Therefore, in the postselection process, their novel features make the wave-packet interference [2] more efficient, resulting in impressive performance, such as higher $R_S$ and postselection probability. It should be pointed out that due to the precoupling, the shape of the meter wave packet is usually largely deformed, especially when the weak value contains the imaginary component, such as $|\phi_p\rangle$ in Fig. 2(b). This effect may complicate the analysis, but its contribution to QFI increase should not be overlooked.

We note that the performance of PWVA is sensitive to the initial state preparation of the meter. Different initial states may lead to quite different QFI. For example, one can easily check that, when $A_w = -20$ and $s = 3$, $Q_I < Q_I^S$ for $\lambda = \pi/4$, while $Q_I > Q_I^S$ for $\lambda = 3\pi/4$. Therefore, it is necessary to explore whether the advantage of PWVA-based metrology is robust to the initial-state preparation. For this purpose, we record the maximum QFI for the initial coherent states $|se^{i\lambda}\rangle$ with $s \in [0, 5]$ and $\lambda \in [0, 2\pi)$ when we scan $|A_w|$ from 5 to 100 with the step 5, and scan the argument of $A_w$ from 0 to $2\pi$ with the step 0.1. As Fig. 3 shows, the QFI is axisymmetric in the phase space and PWVA outperforms WVA potentially in most cases except for initializing the meter to states in the area marked in black, i.e., $\langle p \rangle \approx 0$. Note that for these coherent states an even higher QFI than $Q_I^S$ can be also achieved by replacing $\Omega = p$ with other operators, such as $x$.

Except for QFI, the systematic error plays an important role in precision metrology as well. Equation (6) suggests
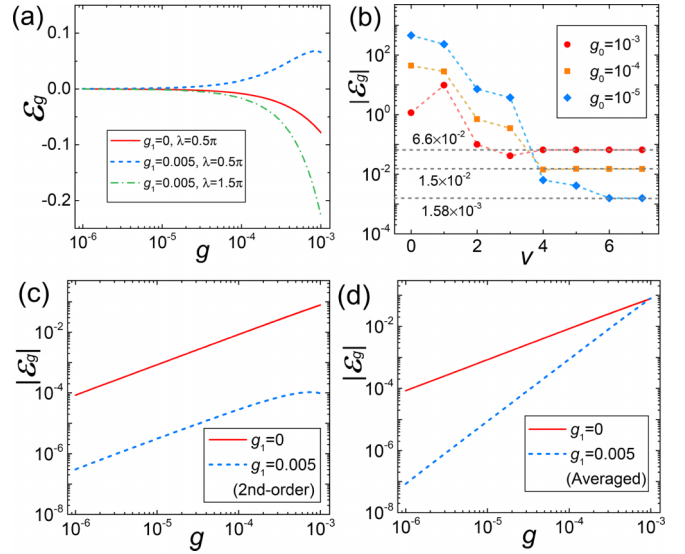


FIG. 4. Relative estimation bias of $g$. (a) The comparison between the relative estimation bias $\varepsilon_g$ of PWVA (blue dashed and green dot-dashed curves) and WVA (red solid curve) methods. To improve the estimation precision, we optimize the PWVA-based metrology by (b) increasing the truncation index $v$ with $g_1 = 0.005, \lambda = 0.5\pi$, (c) taking the second-order approximation of $g$ into consideration with $\lambda = 0.5\pi$, and (d) averaging $g_e$ derived from different initial meter states. The red curves in figures (b)–(d) serve as a comparison. Other parameters used in the calculation are $s = 3, A_w = -20i$, and $v = 6$ [except for (b)].

that the systematic error cannot be reduced by increasing the measurement number $N$. When $N \to \infty$, the first term approaches zero, while the systematic error still remains finite, limiting the performance of PWVA. Thus it is necessary to explore the property of this error in PWVA. For simplicity, in this paper we only consider the estimation bias $g_e - g$, i.e., the difference between the theoretical and estimated value of $g$. Then the relative estimation bias is defined as

$$\varepsilon_g = \frac{g_e - g}{g}, \qquad (23)$$

a quantity resulted from the higher-order approximation with respect to $g$ and $g_1$. In Fig. 4(a), we show $\varepsilon_g$ of both PWVA and WVA schemes for a range of values of $g$ to consider the effect of precoupling on estimation precision. Compared to WVA, the $\varepsilon_g$ of PWVA increases rapidly as $g$ grows, revealing a larger estimation error. This is consistent with the expected conclusion derived from Eqs. (2) and (10) that the estimation precision of PWVA is upper bounded by WVA. Here, we provide three strategies to fight this drawback of PWVA. An obvious approach is to increase $v$ to the interval where the smallest $|\varepsilon_g|$ is obtained, as shown in Fig. 4(b). But this smallest $|\varepsilon_g|$ is limited by WVA, making the accuracy still insufficient. In addition, taking higher-order approximation of $g$ into consideration contributes to the estimation precision as well [Fig. 4(c)]. This method, however, will complicate the theoretical model and make the data processing less efficient. The third strategy is inspired by the fact that the $\varepsilon_g$ derived from states $|\alpha\rangle$ and $|-\alpha\rangle$ have the ability to cancel each other to some extent [Fig. 4(a)] without changing QFI (Fig. 3).

In Fig. 4(d), we display the averaged $\varepsilon_g$ by considering two initial states with $s = 3$ and $\lambda = 0.5\pi, 1.5\pi$. It is clear that this treatment greatly reduces the estimation error of PWVA, and therefore shows the potential in precision metrology.

## V. CONCLUSION AND DISCUSSION

We have considered the feasibility of the PWVA-based precision metrology. By introducing a precoupling process before the WVA scheme, we provide a generalized theoretical model of PWVA to show its advantages over WVA through the metric of QFI. However, several papers show that, in the WVA scheme, formulas of the expectation values and probability densities can be analytically derived if $A$ with special properties is used [40–43]. We here make no assumption of the interaction operators to ensure that the results are compatible with various practical situations, and a linear approximation with respect to $g$ is employed to avoid a verbose expression of QFI. The analysis shows that the PWVA can outperform the WVA in the sensitivity of parameter estimation only if the precoupling operator is properly designed. For example, when the weak value is real, the requirement $[\Omega, \Omega_1] \neq 0$ needs to be met. It is worth noting that $\Omega = \Omega_1$ for the case $A_w/i \in \mathbb{R}$ also leads to an impressive QFI increase, and this special scenario has already been studied in Refs. [38,39]. By tracking the meter wave functions, we find that the mission of precoupling in PWVA is to optimize the state-dependent wave functions into a regime that is most sensitive to parameter $g$. As a result, the shape of the final normalized meter state after postselection is usually deformed, not just shifted from the initial location as in WVA. This difference combined with the postselection probability finally results in a larger QFI to some extent.

However, from Eq. (6), we know that except for QFI, achieving lower systematic error is crucial for parameter estimation as well. Due to the same approximation made about $g$, the estimation accuracy of PWVA is upper bounded by WVA. Then we propose three strategies to fight this shortcoming: increasing the truncation index $v$, taking higher-order approximation of $g$ into account, and averaging the estimation from different initial states. Among them, the third one would be most efficient and deserves the application in precision metrology.

In principle, PWVA can be interpreted as a two-parameter estimation as well if it is used in experiments where the Hamiltonians in two stages of precoupling and interaction are both unknown. Also, the PWVA proposal can be used as a multiparameter estimation with respect to the unknown interaction Hamiltonian only, as the case discussed in Ref. [44]. If the precoupling operation can be properly designed, a desired higher estimation precision may be achieved.

[1] L. Pezzè, A. Smerzi, M. K. Oberthaler, R. Schmied, and P. Treutlein, Rev. Mod. Phys. **90**, 035005 (2018).
[2] Y. Pan, J. Zhang, E. Cohen, C.-W. Wu, P.-X. Chen, and N. Davidson, Nat. Phys. **16**, 1206 (2020).
[3] D. J. Starling, P. B. Dixon, A. N. Jordan, and J. C. Howell, Phys. Rev. A **80**, 041803(R) (2009).
[4] S. Pang and T. A. Brun, Phys. Rev. Lett. **115**, 120401 (2015).
[5] Y. Turek, W. Maimaiti, Y. Shikano, C.-P. Sun, and M. Al-Amri, Phys. Rev. A **92**, 022109 (2015).
[6] S. L. Braunstein and C. M. Caves, Phys. Rev. Lett. **72**, 3439 (1994).
[7] S. L. Braunstein, C. M. Caves, and G. Milburn, Ann. Phys. (NY) **247**, 135 (1996).
[8] L. Zhang, A. Datta, and I. A. Walmsley, Phys. Rev. Lett. **114**, 210801 (2015).
[9] Y. Aharonov, D. Z. Albert, and L. Vaidman, Phys. Rev. Lett. **60**, 1351 (1988).
[10] Y. Aharonov and L. Vaidman, Phys. Rev. A **41**, 11 (1990).
[11] O. Hosten and P. Kwiat, Science **319**, 787 (2008).
[12] J. Dressel, M. Malik, F. M. Miatto, A. N. Jordan, and R. W. Boyd, Rev. Mod. Phys. **86**, 307 (2014).
[13] J. Zhang, C.-W. Wu, Y. Xie, W. Wu, and P.-X. Chen, Chin. Phys. B **30**, 033201 (2021).
[14] P. B. Dixon, D. J. Starling, A. N. Jordan, and J. C. Howell, Phys. Rev. Lett. **102**, 173601 (2009).
[15] C.-W. Wu, J. Zhang, Y. Xie, B.-Q. Ou, T. Chen, W. Wu, and P.-X. Chen, Phys. Rev. A **100**, 062111 (2019).
[16] G. C. Knee and E. M. Gauger, Phys. Rev. X **4**, 011032 (2014).
[17] C. Ferrie and J. Combes, Phys. Rev. Lett. **112**, 040406 (2014).
[18] J. Harris, R. W. Boyd, and J. S. Lundeen, Phys. Rev. Lett. **118**, 070802 (2017).
[19] L. Xu, Z. Liu, A. Datta, G. C. Knee, J. S. Lundeen, Y.-Q. Lu, and L. Zhang, Phys. Rev. Lett. **125**, 080501 (2020).
[20] A. Nishizawa, K. Nakamura, and M.-K. Fujimoto, Phys. Rev. A **85**, 062108 (2012).
[21] A. N. Jordan, J. Martínez-Rincón, and J. C. Howell, Phys. Rev. X **4**, 011031 (2014).
[22] J. Sinclair, M. Hallaji, A. M. Steinberg, J. Tollaksen, and A. N. Jordan, Phys. Rev. A **96**, 052128 (2017).
[23] Y. Kedem, Phys. Rev. A **85**, 060102(R) (2012).
[24] J. Ren, L. Qin, W. Feng, and X.-Q. Li, Phys. Rev. A **102**, 042601 (2020).
[25] S. Pang, Jose Raul Gonzalez Alonso, T. A. Brun, and A. N. Jordan, Phys. Rev. A **94**, 012329 (2016).
[26] S. A. Haine, S. S. Szigeti, M. D. Lang, and C. M. Caves, Phys. Rev. A **91**, 041802(R) (2015).
[27] S. Pang and T. A. Brun, Phys. Rev. A **92**, 012120 (2015).
[28] J. Dressel, K. Lyons, A. N. Jordan, T. M. Graham, and P. G. Kwiat, Phys. Rev. A **88**, 023821 (2013).

[29] C. Krafczyk, A. N. Jordan, M. E. Goggin, and P. G. Kwiat, Phys. Rev. Lett. **126**, 220801 (2021).

[30] G. Strübi and C. Bruder, Phys. Rev. Lett. **110**, 083605 (2013).

[31] J. Martínez-Rincón, W.-T. Liu, G. I. Viza, and J. C. Howell, Phys. Rev. Lett. **116**, 100803 (2016).

[32] L. Qin and X.-Q. Li, arXiv:2207.03668.

[33] J. Huang, Y. Li, C. Fang, H. Li, and G. Zeng, Phys. Rev. A **100**, 012109 (2019).

[34] S. Pang, J. Dressel, and T. A. Brun, Phys. Rev. Lett. **113**, 030401 (2014).

[35] J.-S. Chen, B.-H. Liu, M.-J. Hu, X.-M. Hu, C.-F. Li, G.-C. Guo, and Y.-S. Zhang, Phys. Rev. A **99**, 032120 (2019).

[36] E. Chitambar and G. Gour, Rev. Mod. Phys. **91**, 025001 (2019).

[37] Y. Kim, S.-Y. Yoo, and Y.-H. Kim, Phys. Rev. Lett. **128**, 040503 (2022).

[38] Z.-H. Zhang, G. Chen, X.-Y. Xu, J.-S. Tang, W.-H. Zhang, Y.-J. Han, C.-F. Li, and G.-C. Guo, Phys. Rev. A **94**, 053843 (2016).

[39] P. Yin, W. H. Zhang, L. Xu, Z. G. Liu, W. F. Zhuang, L. Chen, M. Gong, Y. Ma, X. X. Peng, and G. C. Li, Light Sci. Appl. **10**, 103 (2021).

[40] T. Koike and S. Tanaka, Phys. Rev. A **84**, 062106 (2011).

[41] X. Zhu, Y. Zhang, S. Pang, C. Qiao, Q. Liu, and S. Wu, Phys. Rev. A **84**, 052111 (2011).

[42] K. Nakamura, A. Nishizawa, and M.-K. Fujimoto, Phys. Rev. A **85**, 012113 (2012).

[43] Yusuf Turek, H. Kobayashi, T. Akutsu, C.-P. Sun, and Y. Shikano, New J. Phys. **17**, 083029 (2015).

[44] Y. Shikano and S. Tanaka, Europhys. Lett. **96**, 40002 (2011).